## **communications**earth & environment

**ARTICLE** 

Check for updates

1

https://doi.org/10.1038/s43247-023-00773-x

OPEN

# Bedrock mediates responses of ecosystem productivity to climate variability

Xiaoli Dong <sup>1</sup>, Jonathan B. Martin<sup>2</sup>, Matthew J. Cohen <sup>3</sup> & Tongbi Tu <sup>4™</sup>

Sensitivity of ecosystem productivity to climate variability is a critical component of ecosystem resilience to climate change. Variation in ecosystem sensitivity is influenced by many variables. Here we investigate the effect of bedrock lithology and weathering products on the sensitivity of ecosystem productivity to variation in climate water deficit using Bayesian statistical models. Two thirds of terrestrial ecosystems exhibit negative sensitivity, where productivity decreases with increased climate water deficit, while the other third exhibit positive sensitivity. Variation in ecosystem sensitivity is significantly affected by regolith porosity and permeability and regolith and soil thickness, indicating that lithology, through its control on water holding capacity, exerts important controls on ecosystem sensitivity. After accounting for effects of these four variables, significant differences in sensitivity remain among ecosystems on different rock types, indicating the complexity of bedrock effects. Our analysis suggests that regolith affects ecosystem sensitivity to climate change worldwide and thus their resilience.

<sup>&</sup>lt;sup>1</sup> Department of Environmental Science and Policy, University of California, Davis, CA 95616, USA. <sup>2</sup> Department of Geological Sciences, University of Florida, Gainesville, FL 32611, USA. <sup>3</sup> School of Forest, Fisheries, and Geomatics Sciences, University of Florida, Gainesville, FL 32611, USA. <sup>4</sup> Center of Water Resources and Environment, School of Civil Engineering, Sun Yat-Sen University, Guangzhou 510275, China. <sup>™</sup>email: tutb@mail.sysu.edu.cn

limate change has profound impacts on the functioning of Earth's ecosystems<sup>1</sup>. However, our current understanding of ecosystem response to climate change is mostly based on trajectories of mean climate state<sup>2</sup>. This static view neglects how temporal variability of climate may affect ecosystem structure and functioning<sup>3,4</sup>. Because ecosystem responses to climatic variability are a key facet of ecosystem resilience to changing conditions, the characterization of ecosystem sensitivity and the identification of properties that contribute to resilience constitute research priorities of global relevance<sup>5</sup>. Here we investigate how bedrock lithology—including overlying sedimentary properties such as soil thickness and regolith porosity, permeability, and thickness—may affect ecosystem sensitivity to climate variability. The investigation focuses specifically on the direction and magnitude of responses of primary productivity of global terrestrial ecosystems to changes in climate water deficit, a temporally dynamic measure of hydroclimatic variability, applicable worldwide6.

Bedrock lithology can affect the biological productivity of overlying ecosystems through variations in the storage of plantavailable water<sup>7-12</sup>. While bedrock usually has low primary porosity and hydraulic conductivity<sup>13,14</sup>, differences in mineral weathering rates can lead to different rates of regolith formation <sup>15</sup>, regolith permeability and porosity <sup>15</sup>, and production of nutrients needed to support terrestrial ecosystems<sup>8,16</sup>. For instance, carbonate rocks consist of highly soluble minerals, such as calcite and dolomite. These minerals commonly display congruent dissolution by rainwater, forming large voids within the bedrock. Voids coalesce to create preferential flow paths that further enhance dissolution, increase permeability, and limit regolith water retention via leakage<sup>17</sup>. In karst regions, limestone dissolution corresponds directly to elevated calcium concentration in bedrock, with which the regolith water loss rate and ecosystem productivity are strongly correlated<sup>9</sup>. Furthermore, although intact regolith generally has a lower porosity than the more highly weathered soil layer above it, its thickness, commonly tens of meters, allows storage of significant amounts of water<sup>7,10–12,16,18</sup>. Recent studies have shown that water storage within the regolith can be an especially important source for deep-rooted plants during droughts or summer dry seasons, long after shallow soils are dry<sup>19-21</sup>. This deep water source is important because shallow soils, in contrast to weathered bedrock, vary in thickness over a much smaller range and are commonly thin across upland landscapes<sup>22,23</sup>.

While bedrock and regolith properties affect ecosystem productivity<sup>8,9</sup>, we expect that regolith water retention would also affect the sensitivity of ecosystem productivity to climatic variability. Variation in ecosystem sensitivity may be identified as differing magnitudes of productivity changes with water availability, an important aspect of climatic variability. Depending on the primary constraints, ecosystem productivity can respond negatively to climatic water deficit, e.g., drier or warmer conditions decrease ecosystem productivity (Fig. 1). Ecosystem sensitivity can also be positive, where reduced precipitation or warmer conditions lead to enhanced productivity. Previous studies suggest ecosystems in some karst regions exhibit significantly higher sensitivity to interannual temperature and precipitation variations than do surrounding non-karst areas, as a result of lower water holding capacity in karst bedrock9. We expect that regolith properties and bedrock lithology will affect the sensitivity of ecosystem productivity to climatic variability and the specific effects will depend on the primary constraints of ecosystems, e.g., temperature, water availability. In energy-limited ecosystems, low temperature and short growing seasons are primary limitations on ecosystem productivity<sup>24,25</sup>. Longer growing seasons under climatic warming should lead to greater ecosystem water

demand<sup>26</sup>. As such, we expect high water retention capacity in less permeable lithologies to increase ecosystem sensitivity to warming. Conversely, in water-limited ecosystems, we expect low regolith water retention capacity in more permeable lithologies to amplify the sensitivity of productivity to droughts.

Bedrock can also affect ecosystem sensitivity via mechanisms other than water-holding capacity. Bedrock weathering liberates plant-essential nutrients<sup>27</sup>, such P, Ca, Mg, and K, which play a significant role in ecosystem processes and functioning<sup>28,29</sup>. Bedrock minerals can also release toxins (e.g., As, Se, and Cd), which can inhibit plant growth<sup>30</sup>. Furthermore, incongruent weathering of primary clay-forming bedrock minerals can enhance soil production and retention of plant-available nutrients and water<sup>8</sup>. These biogeochemical bedrock properties may alter the sign and magnitude of ecosystem sensitivity to climate water deficit. Their effects of altering ecosystem sensitivity are likely strongest where productivity is not already primarily limited by water<sup>31</sup>.

Here we investigate how soil and regolith water storage mediates responses of ecosystem productivity to climate variability at the global scale. We address three major knowledge gaps: (1) We seek to quantify lithologic effects on the sensitivity of ecosystems to climatic variability in contrast with previous studies that have focused on how lithology affects ecosystem productivity; (2) We use a global framework to evaluate effects of bedrock lithology worldwide rather than limiting our evaluation to local sites or regions; and (3) previous studies have established effects of bedrock geochemistry on ecosystem productivity, but have not isolated the underlying mechanism by explicitly considering the effects of mediating variables (e.g., regolith thickness, permeability, porosity)<sup>8,9,32</sup>. Evaluation of these mediating variables has been previously limited by the paucity of scale-appropriate data, particularly on bedrock permeability and porosity. In this study, we leverage newly available global datasets<sup>6,33–35</sup> to examine the effects of bedrock lithologies and soil and regolith properties on global scale patterns of ecosystem sensitivity. We find a significant effect of properties of bedrock and weathering products on ecosystem sensitivity globally, although the specific effect varies from region to region depending on the primary constraints of an ecosystem.

## Results

Overview of approaches. To evaluate the relationship between lithology and ecosystem sensitivity requires concatenation of multiple global datasets and statistical analysis in two stages. First, we use gridded global measurements of climatic water deficit (CWD; defined as the difference between reference and actual evapotranspiration in mm yr<sup>-1</sup>)<sup>6</sup> and ecosystem productivity inferred from GIMMS (Global Inventory Modeling and Mapping Studies) NDVI (Normalized Difference Vegetation Index) dataset<sup>36</sup>. These two datasets allow us to quantify global patterns of ecosystem sensitivity to climatic variability, as our first-stage analysis. Ecosystem sensitivity in this study is defined as the change in ecosystem productivity, inferred from vegetation greenness captured by NDVI, relative to the change in CWD. Larger absolute values reflect greater sensitivity. Negative sensitivity implies diminished productivity with higher CWD; that is, drying or warming (both increase CWD) reduce ecosystem productivity. In contrast, positive sensitivity implies that increased CWD increases ecosystem productivity. In the secondstage analysis, we use recently available high-resolution data on lithology and hydro-lithological characteristics<sup>33–35</sup> to evaluate effects of bedrock lithology on ecosystem sensitivity quantified in the first-stage analysis.

Preliminary analyses of ecosystem sensitivity suggest that regions of positive sensitivity clustered into desert, tropical, and

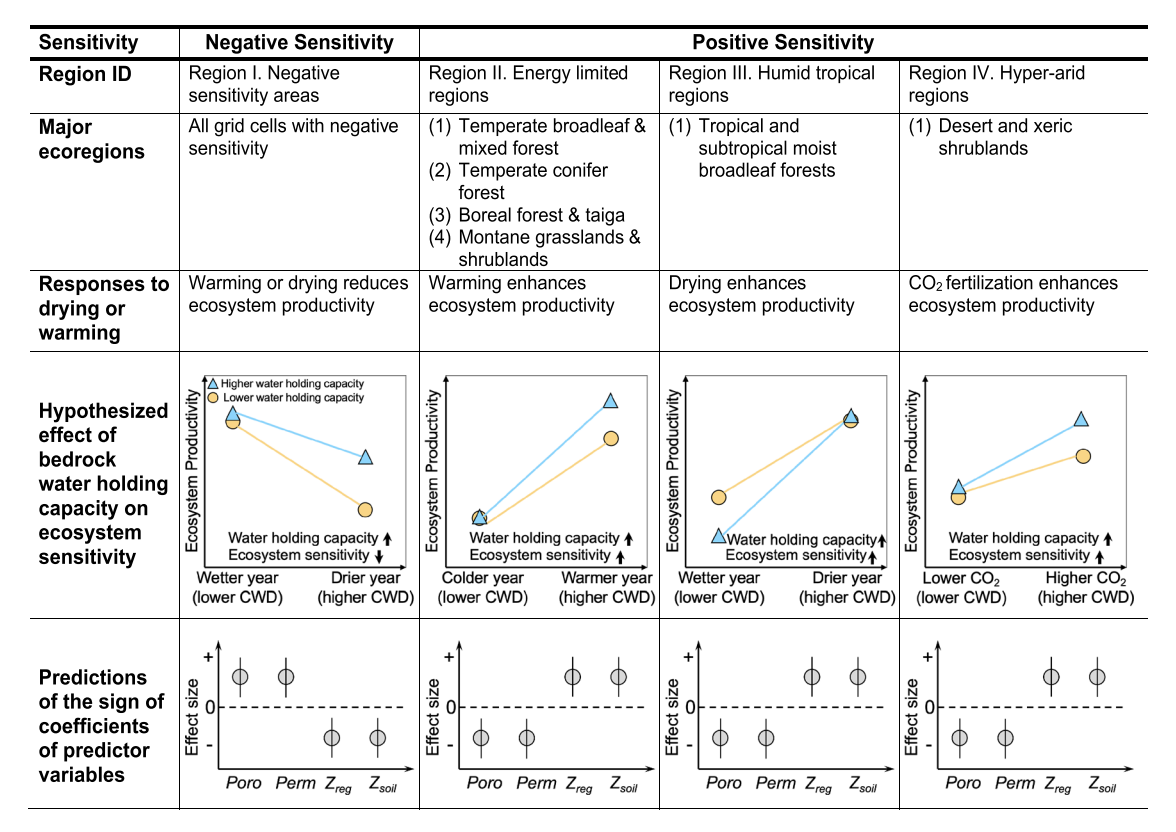


**Fig. 1 Classification of four regions globally and hypothesized region-specific effect of bedrock water holding capacity on ecosystem sensitivity.** The global terrestrial surface is divided into four regions, according to the sign of calculated ecosystem sensitivity and primary constraints of ecosystem productivity for different ecoregions (Table S1; Figs. S1 and S2). We hypothesize that the effect of bedrock water holding capacity on ecosystem sensitivity (steeper slope represents higher sensitivity) varies by region and list predictions of model results (signs of coefficients in Eq. 5) if the hypotheses are supported. "Poro"- porosity, "Perm"- permeability, "Z<sub>Reg</sub>" - thickness of regolith, "Z<sub>soil</sub>" - soil thickness. In the last row: the mean effect size is represented by a circle and vertical lines describe 95% credible intervals of the effect size.

polar regions (Fig. 2). While these regions all show positive sensitivity, as discussed above, the role played by water retention capacity in increasing ecosystem productivity with more severe climatic water deficit might be distinctively different in deserts, tropical regions, and polar regions. The central hypothesis in this study is that bedrock and its properties affect ecosystem sensitivity to climatic variation by mediating ecosystem water retention capacity. These lines of reasoning prompted us to investigate these regions separately. No such zonation was evident for regions of negative sensitivity, which were therefore analyzed as a single group. We thus divided the terrestrial land surface into four regions (Figs. 1 and 2; Table S1; Fig. S1), based first on the sign of estimated sensitivity (i.e., positive and negative  $\alpha$  in Eq. 2 in "4. Methods" below), then, for locations with positive sensitivity, into three energy-limited and water-limited domains. Region I includes all grid cells that showed negative sensitivity, where warming or drying diminishes ecosystem productivity. For regions of positive sensitivity, where warming or drying increases ecosystem productivity, we defined energy-limited regions and water-limited regions. We identified the spatial intersection of grid cells of positive sensitivity and biomes that are primarily energy-limited, including (a) temperate broadleaf & mixed forests<sup>37</sup>, (b) temperate conifer forests<sup>37,38</sup>, (c) boreal forests & taiga<sup>39</sup>, and (d) montane grasslands & shrublands<sup>40,41</sup>, as energylimited regions (or cold regions; Region II) (Figs. S1 and S2). We assume that ecosystems, where productivity is enhanced by lower precipitation, are mostly in humid tropical and subtropical regions<sup>42</sup>. As such, we identified the spatial intersection of locations of positive sensitivity and tropical and subtropical moist

broadleaf forests as Region III. The remaining grid cells with positive sensitivity occur in hyper-arid Saharan desert and Arabian desert and in African tropical and subtropical grasslands, savanna, and shrublands, and are identified as Region IV. A detailed description of the procedure taken to delineate these four regions is provided in Table S1.

Global patterns of ecosystem sensitivity. Globally, the mean sensitivity of ecosystem productivity is 0.00026 (SD = 0.0018) (Table 1; Figs. 2 and 3a); that is, a one unit increase in CWD  $(1 \text{ mm month}^{-1} \text{ for every month in a year, or } 12 \text{ mm year}^{-1})$ leads to a decrease of 0.00026 mean annual NDVI in ecosystem productivity. The range of ecosystem sensitivity is between -0.076 and 0.149, with >99% between -0.01 and 0.01 (Fig. S3). Ecosystem sensitivity also varies with latitude systematically, with positive sensitivity values concentrating in the polar and tropical regions (Fig. 3b). The degree of uncertainty in sensitivity varies greatly among grid cells, and the response of ecosystem productivity to CWD over the 32-year period was statistically significant (95% credible interval excludes zero) in 33.3% of grid cells globally (Fig. 3c, d; Table S2). We note here that the low absolute values of ecosystem sensitivity are only arbitrary (a matter of unit); the focus of this study is to explain the spatial variation of ecosystem sensitivity.

We found a negative relationship between CWD and productivity for most ecosystems (63% of grid cells, of which 45% were statistically significant), with a mean sensitivity of -0.0009. The negative value indicates the inhibitory effects of high CWD on ecosystem productivity. Notably, 75% of grid cells with statistically

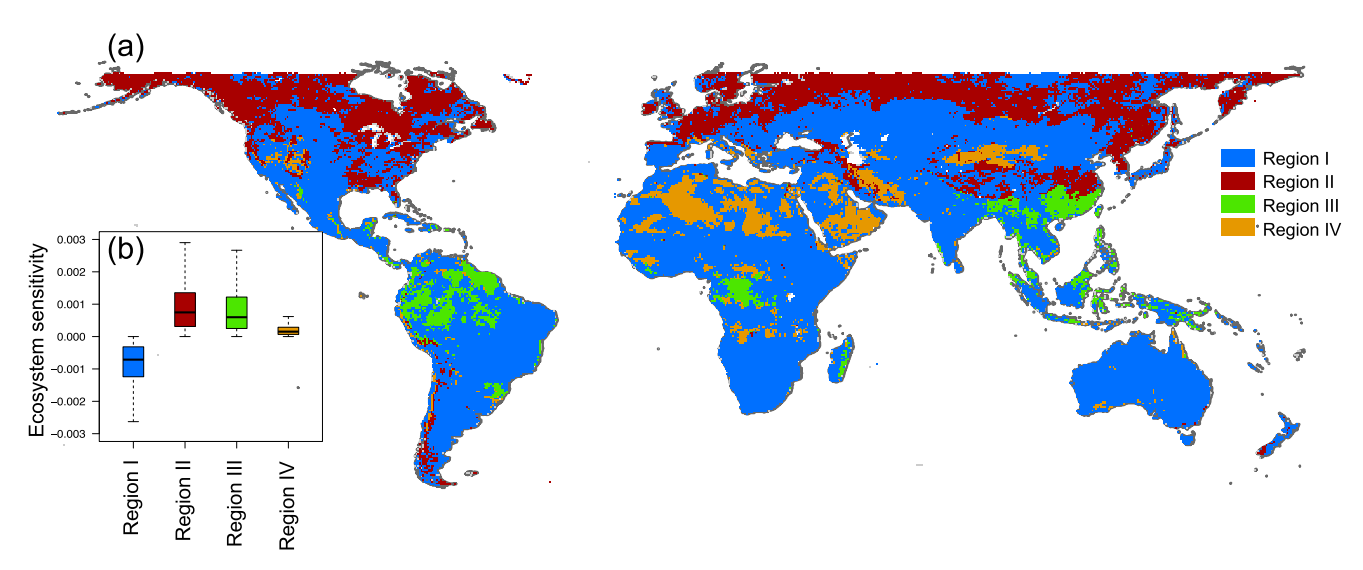


**Fig. 2 Delineation of regions of global terrestrial surface. a** Four regions are delineated in this study. Region I denotes areas of negative sensitivity; regions with positive sensitivity include Region II where energy limitation is likely, Region III denoting humid tropical regions, and Region IV denoting desert and xeric regions. Detailed definitions of each region are provided in Fig. 1. **b** Distribution of ecosystem sensitivity values by region. Box plots: box limits show the first quartile (Q1) and third quartile (Q3); central line inside the box represents the median ecosystem sensitivity of a given region; and the segments at ends indicate (Q1–1.5 interquartile range) and (Q3 + 1.5 interquartile range).

	All grid cells		Grid cells with statistically significant sensitivity	
	Maximum sensitivity	Mean (standard deviation)	Maximum sensitivity	Mean (standard deviation)
Region I. Negative-sensitivity region	-0.076	-0.00093 (0.0014)	-0.076	-0.0026 (0.0029)
Region II. Energy-limited region	0.077	0.0011 (0.0017)	0.077	0.0033 (0.0033)
Region III. Humid tropical region	0.149	0.0010 (0.0032)	0.149	0.0032 (0.0074)
Region IV. Desert and xeric shrublands of positive sensitivity	0.0035	0.00022 (0.00025)	0.0035	0.0023 (0.00062)
Global	0.149	-0.00026 (0.0018)	0.149	-0.00050 (0.0044)

significant sensitivity were moderately water-limited biomes, including (1) tropical and subtropical dry broadleaf forests, (2) tropical and subtropical grasslands, savanna, and shrublands, (3) temperate grasslands, savanna, and shrublands, (4) temperate conifer forests, (5) Mediterranean forests, woodlands, and scrubs, and (6) desert and xeric shrublands (Figs. 3c and S2).

In contrast, 37% of ecosystems exhibited a positive relationship between ecosystem productivity and CWD, of which 13.3% were statistically significant (Fig. 3). Of the areas where ecosystem sensitivity was positive, 63% were in the energy-limited regions (Region II), 20% in desert and xeric shrublands (Region III), and 14% in humid tropical regions (Region IV; tropical and subtropical moist broadleaf forests) (Figs. 3 and S2). Energy-limited regions refer to ecosystems that are primarily limited by cold temperatures and a short growing season, e.g., high latitude areas (boreal forests and taiga)<sup>25</sup>, high-altitude areas (montane grasslands and shrublands and montane alpine and subalpine forests)<sup>24</sup>, and temperate broadleaf and mixed forests that are located in higher-latitude areas<sup>43</sup> (Fig. S2). Both energy-limited regions (mean = 0.0011) and humid tropical regions (mean = 0.0010) were characterized by relatively high sensitivity and large spatial variation (Table 1; Fig. 3). Although sensitivity in desert and xeric shrublands (Region IV) is also positive, the values are approximately an order of magnitude lower than the other regions (Table 1; Fig. 3).

The positive sensitivity in energy-limited regions means that higher CWD, likely due to increased temperatures, increases ecosystem productivity. Humid tropical regions (tropical & subtropical moist broadleaf forests) near the equator (Fig. S2) also show a positive sensitivity. In contrast with cold regions where ecosystem sensitivity depends on temperature, a higher CWD in tropical settings likely results from decreased annual precipitation, which enhances ecosystem productivity. This rainfall control aligns with previous studies showing increased productivity in humid tropical ecosystems with reduced precipitation<sup>44,45</sup>. Desert and xeric shrublands that show positive sensitivity are primarily located in hyper-arid regions including the Arabian and Sahara deserts, and Saharan xeric steppe and woodland (Figs. 3 and S2). A positive relationship suggests that productivity of deserts and xeric shrublands in certain hyper-arid regions increases with warming, consistent with the greening observed in dryland foliage cover since the  $1980s^{46-48}$ .

Effects of regolith permeability and porosity on ecosystem sensitivity. In regions of negative sensitivity, regolith porosity, and permeability significantly increase ecosystem sensitivity, that is, ecosystems located on high permeability and porosity regolith

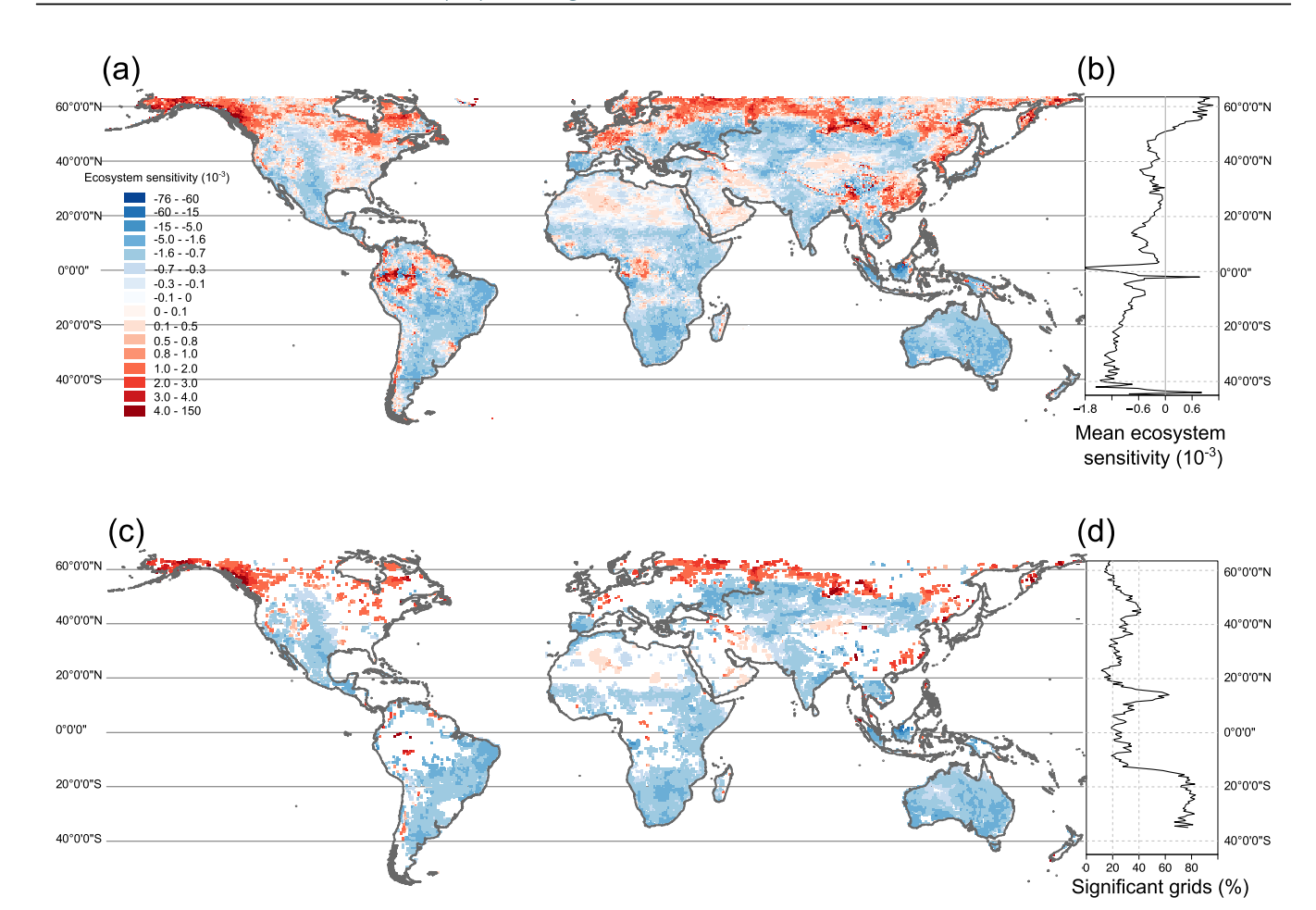
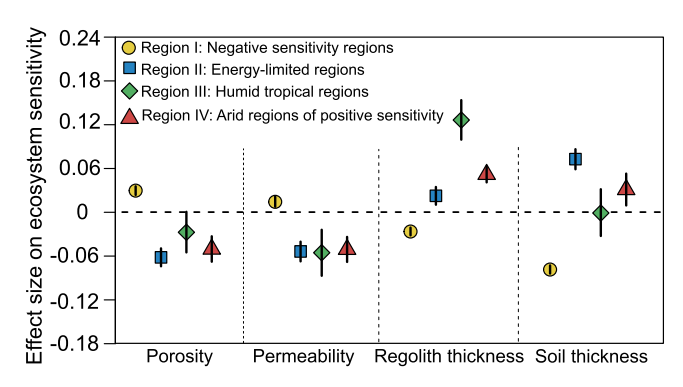


Fig. 3 Sensitivity of ecosystem productivity to variability in climatic water deficit (CWD) between 1982 and 2013 globally. a Shows calculated sensitivity values for the global terrestrial surface; c shows sensitivity values in locations where ecosystem sensitivity values are statistically significant (95% credible interval does not contain zero). b shows the mean ecosystem sensitivity by latitude and d shows the proportion of grid cells at each latitude where sensitivity values are statistically significant. Positive sensitivity (shades of red) implies increased ecosystem productivity in response to higher CWD, while negative values (shades of blue) suggest diminished productivity with higher CWD (i.e., drying, warming, or both).



**Fig. 4 Effect size of variables describing the properties of bedrock and its products on ecosystem sensitivity for four regions.** Effect size of each variable is inferred by the mean (denoted by circles, squares, diamonds, and triangles) and 95% credible interval (denoted by the vertical line) of posterior estimates of regression coefficients from the model. Definitions of four regions are provided in Fig. 1 and Table S1.

are more responsive to climatic variability (Fig. 4). Statistical correlations from the model suggest that in regions of positive sensitivity, permeability, and porosity might also exert significant effects. In energy-limited areas, increased regolith porosity and permeability significantly reduce the enhancement effect of warming on productivity (Fig. 4). Similarly, in the desert and

xeric shrublands of hyper-arid regions, high permeability and porosity dampen productivity enhancement by CWD. Finally, in humid tropical regions, ecosystems located on regolith of lower permeability or porosity are more responsive to a drier climate (Fig. 4).

In regions of negative sensitivity, a one SD increase in permeability (i.e., change in permeability  $\log(k)$  by ~0.96) or porosity leads to an increase of 3 and 7% relative to mean regional sensitivity. In energy-limited regions, a one SD increase in porosity or permeability results in decreases of sensitivity by 13 and 12% relative to the regional mean level. In humid tropical regions, an increase of one SD in porosity or permeability decreases sensitivity by 6 and 12% relative to the regional mean level. Finally, in hot deserts of positive sensitivity, a one SD increase in porosity or permeability decreases sensitivity by 11% relative to the regional mean. In summary, a change of one SD from the region-specific mean in regolith porosity and permeability results in changes in sensitivity by 3% ~ 13% of the region-specific mean.

Effects of regolith and soil thickness on ecosystem sensitivity. In regions with negative sensitivity, both increasing regolith and soil thickness reduce ecosystem sensitivity (Fig. 4). An increase of one SD in soil and regolith thickness reduces ecosystem sensitivity by 17 and 6% of the regional mean level, respectively. For regions with positive sensitivity, the effects are most significant.

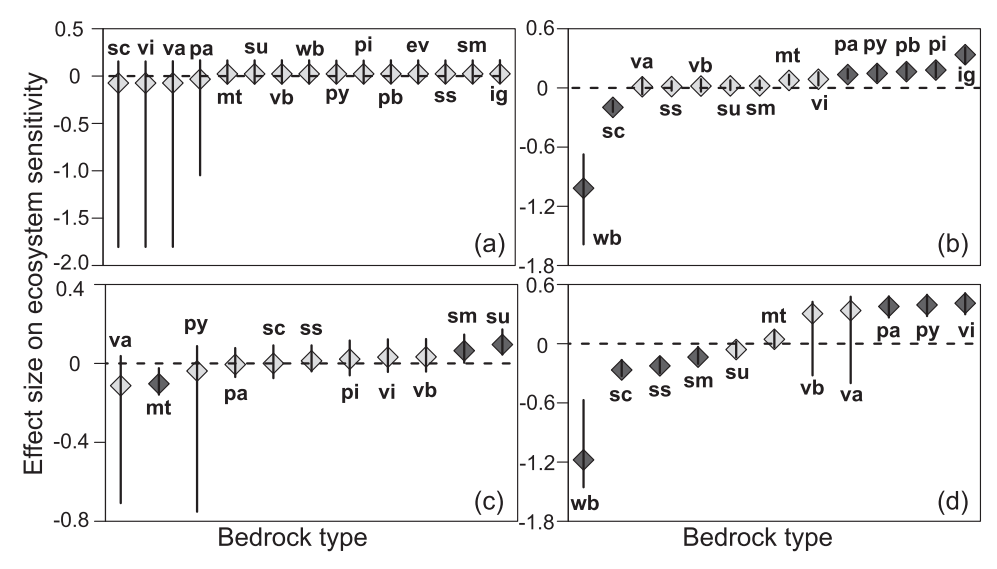


**Fig. 5 Effect size of different types of bedrock lithology on ecosystem sensitivity in different regions. a** Region I. Negative-sensitivity regions; **b** Region II. Energy-limited regions; **c** Region III. Humid tropical regions; and **d** Region IV. Hyper-arid regions of positive sensitivity. Statistically significant effects are in black and those not significant are in gray. Bedrock class: "ev"- evaporites, mt metamorphic rocks, "pa"- acid plutonic rocks, "pb"- basic plutonic rocks, "pi"-intermediate plutonic rocks, "py"- pyroclastics, "sc"- carbonate sedimentary rocks, "sm"- mixed sedimentary rocks, "ss"- siliciclastic sedimentary rocks, "su"- unconsolidated sediments, "va"- acid volcanic rocks, "vb"- basic volcanic rocks, "vi"- intermediate volcanic rocks, "wb"- water bodies. The number of bedrock types is different among regions because not all lithology categories exist in each region. Diamond symbols denote the posterior mean values and the vertical lines denote the 95% credible intervals of the estimated mean.

In energy-limited regions, a one SD increase in regolith thickness and soil thickness increases the responsiveness of ecosystem productivity to warming by 5 and 18% of the regional mean. Similarly, thicker regolith in humid tropical regions enhances the positive response of productivity to higher CWD; however, the effect of soil thickness was not statistically significant (Fig. 4). In these ecosystems, a one SD increase in regolith thickness increased sensitivity by 34% of the mean. For ecosystems in the desert and xeric landscapes of positive sensitivity, a one SD deviation in regolith and soil thickness enhances sensitivity by 12 and 7% of the mean level, respectively. In summary, a change of one SD from the region-specific mean in regolith thickness and soil thickness results in changes in sensitivity by 6%~34% of the region-specific mean.

Residual effects of bedrock lithology. The 15 lithological classes used are distinguished by their global variation based on weathering and hydrological studies ("hydrolithology")49. After controlling for effects of soil thickness and regolith porosity, permeability, and thickness, soil thickness, residual effects of lithology were not significant in regions with negative sensitivity (Fig. 5a); however, significant random effects of lithology on ecosystem sensitivity remained in regions with positive sensitivity (Fig. 5b-d). Notably, sedimentary bedrock, including mixed sedimentary bedrock (mixed siliciclastic-carbonate rocks), carbonate sedimentary rocks, siliciclastic sedimentary rocks, and unconsolidated sediments, show significantly different effects on ecosystem sensitivity than other rock types (Fig. 5b-d). Sedimentary rocks dampen the positive productivity response to CWD in energy-limited regions (Fig. 5b) and in the desert and xeric regions (Fig. 5d), while pyroclastics and acid plutonic rocks intensify ecosystem sensitivity to CWD in those regions (Fig. 5b, d). Sedimentary bedrocks however increase ecosystem sensitivity in humid tropical regions (Fig. 5c). In energy-limited regions, ecosystems located on plutonic rocks overall show greater productivity increases under warming (Fig. 5b).

#### Discussion

Sensitivity of ecosystems productivity to climatic variability varies widely, both in sign and magnitude (Fig. 3)4. Most of Earth land surface (~63%) shows a negative sensitivity to CWD, suggesting that the dominant effect of drying or warming is to reduce ecosystem productivity (Fig. 3). Despite being limited to a much smaller spatial extent, the magnitude of positive sensitivity of ecosystems in energy-limited and in humid regions is slightly higher (Table 1; Fig. 2). While ecosystems in some deserts and xeric shrublands in hyper-arid regions also exhibit positive sensitivity, its magnitude is much lower than other regions (Table 1; Fig. 2). Furthermore, we found that 45% of grid cells in negative sensitivity regions are statistically significant, compared to only 13% for positive sensitivity regions. This difference suggests that positive effects of climatic drying or warming on ecosystem productivity is far more variable than their negative effects. Spatial distribution of ecologically sensitive regions identified in this study is remarkably consistent with previous studies using different sensitivity metrics<sup>4,44</sup>, supporting the robustness of the pattern revealed in our study. Variability of ecosystem sensitivity has previously been suggested to be affected by many ecosystem attributes, such as species niche partitioning<sup>50</sup>, biodiversity<sup>51,52</sup>, ecosystem successional stage<sup>53</sup>, and landscape topography<sup>54</sup>. Our study suggests that at the global scale, properties of bedrock and its weathering products also have a significant effect on ecosystem sensitivity to climatic variability. This effect occurs primarily through modifications of the water-holding capacity of bedrock and its products. Effects of modifications can vary among geographic regions, depending on primary constraints (e.g., water, temperature, nutrients) of ecosystem productivity in each region. Across all regions, properties of bedrock weathering products exert a relatively strong effect on ecosystem sensitivity (Fig. 4). A change of one SD in regolith porosity and permeability results in a 3% ~ 13% change in ecosystem sensitivity, and a change of one SD in soil thickness and regolith thickness leads to a 6% ~ 34% change in sensitivity, depending on the region.

Increased regolith permeability reduces water holding capacity of the subsurface of an ecosystem. As a result, ecosystem productivity can become sensitive to CWD accompanied by limited hydrologic buffering capacity. In ecosystems where productivity declines with intensified CWD, i.e., in regions of negative sensitivity, as expected, we find that high regolith permeability and porosity amplify ecosystem sensitivity to climatic variability (Fig. 4). Previous studies have highlighted the importance of soil water storage capacity in affecting water availability and partitioning<sup>55,56</sup>, although a few empirical studies suggest that soil thickness is not evidently related to plant water availability<sup>32</sup>. Soils are commonly thin (<0.5 m) across most upland landscapes, and vary in thickness over a smaller range compared to regolith thickness<sup>22,23</sup>. Regolith below soils has been increasingly recognized to be also important to ecohydrological variability 11,20 and regolith water retention can be more important for plants than soil water, especially during droughts. For instance, in Mediterranean-type ecosystems, roots of ponderosa pine (Pinus ponderosa) seedlings penetrate through the soil and encounter weathered bedrock within the first two years after germination, and regolith supplies at least 70% of plant water use during the growing season<sup>20</sup>. However, our results suggest that, at the global scale both regolith and soil thickness significantly reduce ecosystem sensitivity in water-limited regions, with greater effects attributed to soil thickness in most areas (Fig. 4).

Both model predictions and empirical observations have shown that tropical drying leads to increased ecosystem productivity<sup>57–59</sup>. Results from this study further support that pattern (Figs. 3 and S4). The positive ecosystem sensitivity of this region reflects reduced ecosystem productivity with elevated precipitation, which can result from several mechanisms. Higher rainfall reduces the diffusion of oxygen through water-filled soil pores, leading to oxygen limitation of roots and heterotrophic microbes<sup>60</sup>. While oxygen limitation may not appear to affect plant growth directly, slower decomposition rates can decrease nutrient regeneration and limit the nutrient supply for plant growth<sup>61</sup>. In addition to nutrient leaching, this limitation may be exacerbated by light limitation, as precipitation and associated cloud cover reduce light availability. We expect areas of higher water-holding capacity to be more severely suppressed by excessive water, and thus in those areas, primary productivity should exhibit a stronger response to reduced precipitation than in areas of lower water-holding capacity (Fig. 1). This hypothesis is supported by our results that indicate a stronger productivity response to drying by ecosystems located on bedrock of lower permeability and porosity than those on more permeable and porous bedrocks (Fig. 4). Similarly, we expect ecosystems located on thicker soils and thicker regolith to be suppressed more by excessive precipitation. This suppression is due to greater water storage capacity of thicker soil and regolith, hence a stronger response to drying (Fig. 4). It is important to note, however, that humid tropical ecosystems undergo complex biogeochemical transitions under climatic drying<sup>62</sup>. Underlying mechanisms to explain the correlation between soil/regolith thickness and ecosystem sensitivity are likely manifold.

The primary limitations on ecosystem productivity in energy-limited regions are low temperatures and short growing seasons<sup>24,25</sup>. Recent increases in summer temperatures have enhanced rhizome growth and leaf production by up to threefold in alpine and subalpine plants<sup>24</sup>. Similarly increased productivity is reflected in steady increases in carbon sequestration by boreal forests<sup>63</sup>. Although warming can enhance ecosystem productivity (Figs. 3 and S4), warmer temperatures also elevate evapotranspiration and alter precipitation regimes<sup>26</sup>. These changes in water balance may limit water availability, and productivity enhanced by a longer growing season can be reduced or even offset

by water limitation. During the warm 2005–2015 period in alpine and subalpine forests, growth began to broadly decrease, likely due to intensified water shortages<sup>24</sup>. Similarly in boreal forests, warming releases plants from cold limitation but can induce water shortages, which then limit productivity increases by higher temperatures and longer growing seasons<sup>64</sup>. Water limitation of productivity during warming may be reduced in areas with low regolith permeability and porosity and thicker regolith and soils, because of the elevated water retention capacity of these areas (Fig. 4).

Significantly enhanced productivity in response to increased CWD was found in hyper-arid regions and other water-limited regions, concentrated in deserts and xeric shrublands in Sahara and Sahel areas and the Arabian Peninsula and tropical & subtropical grasslands, savanna, and shrublands south of Sahel (Figs. 3 and S2). Enhanced productivity in arid regions has been hypothesized to be caused by a fertilization effect of elevated atmospheric CO<sub>2</sub><sup>48,65</sup> coupled with increased precipitation since the early 1980s<sup>66,67</sup>, even though CWD has risen since the late 1950s in this region (Fig. S5). As ecosystems in these areas are highly water limited, we suspect that the correlation between CWD and atmospheric CO<sub>2</sub> caused the spurious positive correlation between ecosystem productivity and CWD (Fig. S5). If elevated atmospheric CO<sub>2</sub> is the root cause for enhanced productivity, increased water holding capacity should allow water-limited ecosystems to respond more vigorously to higher atmospheric CO2 in these arid landscapes (Fig. 1). Furthermore, previous studies suggest that soil water is a dominant driver of ecosystem change in African drylands<sup>68</sup>. Conforming to our expectation, the thickness of soil and regolith significantly enhances ecosystem sensitivity, and a higher regolith porosity and permeability suppress the effect of CO<sub>2</sub> fertilization on ecosystem productivity (Fig. 4).

Significant residual effects of bedrock lithology on ecosystem sensitivity, particularly where underlain by sedimentary rocks (Fig. 5), suggest water holding capacity is not the only principal control on ecosystem sensitivity. In the 12 largest mid-latitude karst regions in the Northern Hemisphere, six show significantly lower ecosystem sensitivity to temperature, and four show significantly higher sensitivity, compared to adjacent non-karst areas<sup>9</sup>, reflecting the complexity of the effects of bedrock lithology. One way in which bedrock type may affect productivity is through contributions of nutrients from bedrock mineral weathering. Different rock types will have significantly different phosphate<sup>69</sup> and nitrogen concentration<sup>70</sup>, which significantly affect nutrient availability in soils. For instance, carbonate rocks and mixed siliciclastic-carbonate rocks have low phosphate content<sup>69</sup>, which could induce nutrient limitation of plant growth<sup>71</sup>. The strong nutrient limitation will likely reduce the plant growth response to other resources, such as dampened sensitivity to water availability<sup>31</sup>. As plants adapt to the relatively high hydrological variability in regions of sedimentary bedrock, their sensitivity to water stress may in fact become low, as has been reported in the case of plant adaptation to variability in rock-derived nutrients<sup>72,73</sup>. We emphasize that the mechanisms hypothesized here are based only on statistical correlations and causal inferences are speculative. Further research controlling explicitly for confounding variables would be required to elucidate underlying mechanisms with greater certainty.

Several aspects of this study can be refined. We did not explicitly correct for agricultural areas, whose productivity is largely controlled by humans and thus tends to be more stable than unmanaged terrestrial ecosystems. This would dampen the ecosystem sensitivity we calculated at the grid scale. Given the relatively small ratio of croplands to unmanaged lands and the significantly strong sensitivity to climatic variability we observed (Fig. 3), our conclusion on the effect of lithology in this study is unlikely to be significantly altered; but still, anthropogenic

activities need to be taken into consideration to better quantify ecosystem sensitivity. Our study quantifies the relative sensitivity of ecosystem productivity to climate variability over a 32-year period, as a component of ecosystem resilience. Results suggest that the properties of bedrock and associated regolith and soil have a significant effect on ecosystem responses to climatic variability, mainly through their control of water holding capacity. The impact of bedrock properties on ecosystem sensitivity is considerable (~30%) given the global scale of the analysis. A direct comparison of the explanatory power of other covariates (e.g., biodiversity<sup>51</sup>, landscape topography<sup>54</sup>) for ecosystem sensitivity is still needed, but is not yet feasible given the lack of existing studies at these same scales. Our global scale analysis suggests that terrestrial ecosystem functioning is determined not only by atmospheric, biospheric, and pedospheric properties and their interactions, but also by the properties of the weathered portion of the lithosphere, specifically soils and regolith. This generalization is global in scope, despite a rich regional variation in proximal mechanisms and their magnitudes.

#### Methods

**Data compilation for estimating ecosystem sensitivity.** All datasets used in this study are standardized to be annual temporal resolution and 0.5° (longitude) by 0.5° (latitude) spatial resolution. Where the temporal resolution of the source data was finer than annual, we calculated and analyzed annual means. Where source data spatial resolution was finer than 0.5°, we obtained grid cell means by bilinear interpolation. The temporal coverage of the study is from 1982 to 2013, a 32-year period, and the spatial coverage is the entire land surface between 180°W–180°E and 55°S–90°N

To estimate the sensitivity of ecosystem productivity to climatic variability, we combined satellite records of the normalized difference vegetation index (NDVI) with globally gridded climatic water deficit (CWD). NDVI has an unparalleled continuous global time series, and relates strongly to leaf area, fraction of absorbed photosynthetically available radiation, gross primary productivity, and many other more advanced vegetation indices<sup>74–77</sup>. Our NDVI time series was derived based on the GIMMS NDVI dataset at 1/12° spatial resolution and 15-day temporal resolution, from which we calculated mean annual NDVI at 0.5° resolution. The processed NDVI is used to represent annual ecosystem productivity. The selected dataset is obtained from AVHRR series<sup>36,78</sup>, which has gone through atmospheric correction, geometric rough correction, geometric fine correction, and correction for impact of volcanic eruptions, and has been processed for short-term effects of atmospheric aerosols and cloud cover to ensure quality.

Climatic water deficit is defined as the difference between reference and actual evapotranspiration based on the one-dimensional modified Thornthwaite-Mather climatic water-balance model<sup>79,80</sup>. CWD exerts strong control over the spatial distribution of plant functional types and is an important driver of ecosystem productivity<sup>81</sup>. It is more directly linked to ecosystem productivity and water resources than precipitation and temperature alone since it accounts for combined effects of water and energy<sup>6</sup>. The recent TerraClimate<sup>6</sup> dataset provides high-resolution (1/24°, ~4 km) monthly CWD estimates (mm month<sup>-1</sup>) for the global terrestrial surface area from 1958–2020 (Fig. S6). We rescaled these observations to 0.5° resolution and calculated annual CWD (by taking average of the original monthly CWD for a given year) between 1982 and 2013.

Calculating grid-specific ecosystem sensitivity. We defined "ecosystem sensitivity" here as the change in NDVI caused by a unit change in CWD, ranging from positive to negative infinity. This definition captures the sensitivity of ecosystem primary productivity, approximated by NDVI, to the interannual variability of CWD. Negative sensitivity implies that lower CWD increases ecosystem productivity, and positive sensitivity implies that ecosystem productivity increases with CWD.

For each grid cell, we first constructed a Bayesian linear regression between CWD and NDVI (both were first detrended) to describe the local productivity-climate relationship. A total of 49,389 regressions (grid cells) were performed spanning all land grid cells in the study domain. At each grid cell i, we assumed that mean annual NDVI follows a normal distribution (likelihood function) with mean  $\mu_i$  and variance  $\tau$ :

$$NDVI_t \sim Normal(\mu_t, \tau)$$
 (1)

where t is the index of year (t = 1, 2, ..., 31, 32). The model for the estimated mean,  $\mu_t$  (Eq. 2), is expressed as:

$$\mu_t = \alpha_0 + \alpha \times CWD_t \tag{2}$$

These fitted slopes ( $\alpha_i$ ) define the sensitivity of ecosystem productivity (NDVI) at the grid cell i to interannual variability of CWD. Such a statistical representation

of ecosystem climatic sensitivity is consistent with definitions in the literature  $^{44,82,83}$ . The standard deviation of the fitted slope  $(\sigma_i)$  describes the uncertainty of the estimated sensitivity. We computed the statistical significance of ecosystem sensitivity based on whether the 95% credible intervals of the posterior distribution of  $\alpha_i$  contain zero. We retained all regression coefficients (sensitivity values), regardless of statistical significance to preserve the information contained in data from all grid cells. In the second-stage of our analysis, we use hydrogeochemical variables to explain the variation in sensitivity calculated here. However, the calculated sensitivity values are associated with different levels of uncertainty among grid cells, captured by  $\sigma_i$ . We used  $\sigma_i$  as weights for the relative effect of a given grid cell in estimating parameters in the second-stage modeling. This is described in more detail below in "2.5. Statistical models to explain variation in ecosystem sensitivity."

Data compilation for explanatory variables. Five variables that are used to explain the variation of ecosystem sensitivity computed above include bedrock lithology class, regolith porosity, regolith permeability, soil thickness, and regolith thickness. Bedrock classes are from the high-resolution global lithological map database GLiM<sup>33</sup>, which represents the rock types of the Earth surface across 1,235,400 polygons. The lithological classification has three levels. The first level contains 15 broad lithological classes: evaporites, ice and glaciers, metamorphics, acid plutonic rocks, basic plutonic rocks, intermediate plutonic rocks, pyroclastics, carbonate sedimentary rocks, mixed sedimentary rocks, siliciclastic sedimentary rocks, unconsolidated sediments, acid volcanic rocks, basic volcanic rocks, intermediate volcanic rocks, and water bodies. This classification is not based on conventional rock classification ("geo"-oriented lithology), but rather on the sensitivity of rocks to chemical and mechanical weathering and their eventual transport via surface water ("hydro"-oriented lithology)<sup>49</sup>. The second level contains 12 additional classes and the third level includes 14 subclasses, describing more specific rock attributes<sup>33</sup>. The first level aligns with the purpose of this study and was used for all analyses presented here.

Regolith porosity and permeability were obtained from the Global HYdrogeology MaPS (GLHYMPS) $^{34}$ , which contains permeability and porosity of consolidated and unconsolidated geologic units below soil horizons (hydrolithologies), with an average polygon size of  $\sim 100 \, \mathrm{km^2} \, ^{34,84}$ ; this was upscaled to 0.5° by 0.5°. Permeability, the ease of fluid flow through porous media, serves as a fundamental control on subsurface flow at all depths. Porosity is the fraction of rock or sediment that is void space, and thus controls subsurface water storage capacity. For each bedrock type, porosity and permeability are generally positively but nonlinearly correlated $^{85}$  (Fig. S7). The global geological datasets we analyze include a large set of bedrock lithologies under a wide variety of physical conditions. As a result, the correlation coefficient is only 0.03 between regolith porosity and permeability, indicating that these two variables yield complementary and independent information.

Data on soil and regolith thicknesses are from a high-resolution (30 arcseconds or ~1 km) global gridded dataset describing the thickness of high-porosity material above unweathered bedrock<sup>35</sup>. The dataset includes soil thickness, intact regolith thickness, and sedimentary deposits based on topography, climate, and geology inputs, with sites partitioned into upland and lowland landscape components, based on net erosion vs. deposition over geological time scales (~105 years and longer). In uplands, high-porosity materials are termed regolith, which is divided into soil and underlying intact regolith. The intact regolith layer refers to the chemically altered but relatively immobile materials between the mobile soil layer and unweathered bedrock<sup>18</sup>. Upland soil thickness varies from as little as few decimeters to a few meters, while intact regolith thickness typically varies from a few meters to tens of meters. In lowlands, all unconsolidated materials above bedrock are classified as sedimentary deposits, with thickness from tens to hundreds of meters<sup>35</sup>. Estimated soil, intact regolith, and sedimentary deposit thickness are limited to 0-50 m<sup>35</sup>, which is the most relevant range for plant rooting depths in terrestrial ecosystems. In this study, "regolith" refers to the intact regolith layer, and "soil" is defined as soils in uplands or unconsolidated sediment deposits in lowlands.

Statistical models to explain variation in ecosystem sensitivity. The secondstage model seeks to explain the variation in ecosystem sensitivity ( $\alpha_i$  in Eq. 2) across grid cells. In this stage, the estimated sensitivity (a) and the standard deviation of the sensitivity ( $\sigma$ ) are treated as "data" or known quantities. We used a weighted Bayesian hierarchical regression<sup>86</sup>, so that each sensitivity value is 'weighted' according to its variance estimated from the model in the first-stage,  $\sigma^2$ .  $\sigma^2$  can be interpreted as how reliable the estimated ecosystem sensitivity is (or how strong the coupling of CWD and NDVI is). This method discounts grids whose estimated ecosystem sensitivity is highly uncertain and allows us to use maximum amount of information contained in the full dataset. It provides the strongest model inference of parameter values. Grid cells whose sensitivity values are more statistically significant (smaller  $\sigma$ ) exert a larger influence on the statistical inference of the effect of underlying drivers on sensitivity than grid cells whose sensitivity values are only marginally significant or not statistically significant (larger  $\sigma$ ). Since a high sensitivity is defined as  $\alpha$  that deviates far from 0, i.e., very negative values or very positive values, we took the absolute values of all original  $\alpha$ , so that large values consistently represent high sensitivity. We used a link function of log

transformation so that the range of the sensitivity extends from negative to positive infinity. The model also controls for spatial autocorrelations ( $K_{ij}$ ), which might introduce unobserved (latent) processes that simultaneously affect the explanatory variables and the outcome variable. The likelihood of the data, that is, the estimated ecosystem sensitivity from models in the first-stage, is described as:

$$\log(|\alpha|) \sim \text{MVNormal}(\mu 2, \mathbf{K})$$
 (3)

$$K_{ij} = (\sigma_i \sigma_j) \eta^2 \exp\left(-\rho^2 D_{ij}\right) \tag{4}$$

where i donates grid cell ID (i=1,2,...,49,389). **K** is a variance-covariance matrix, represented by a Gaussian process kernel. **K** accounts for the spatial autocorrelation of ecosystem sensitivity among grid cells located nearby. The covariance between any pair of grid cells i and j is  $K_{j\bar{p}}$ , which is defined by Eq. 4.  $D_{ij}$  is the distance (in meter) between grid cell i and j and the parameter  $\rho$  describes the rate of decline of the covariance between grid cell i and j with distance. If  $\rho$  is large, covariance declines rapidly with distance.  $\eta^2$  is the maximum covariance between any two grid cells. Theoretically, the dimension of D is 49,389 ×49,389. For computational efficiency, we assume that autocorrelation is zero (i.e., grid cells are independent) beyond a distance of 1000 km (~ twenty 0.5° grid cells).

We define the model for the predicted sensitivity as a linear regression on bedrock-related properties and bedrock lithology:

$$\mu 2_{i} = \beta_{0} + \beta_{1,reg(i)} Por_{i} + \beta_{2,reg(i)} Perm_{i} + \beta_{3,reg(i)} RegZ_{i} + \beta_{4,reg(i)} SoilZ_{i} + \varepsilon_{bedrock,reg(i)}$$
 (5)

where Por and Perm denote porosity and permeability of the intact regolith, respectively, RegZ refers to mean regolith thickness in a grid, and SoilZ is the thickness of soil and unconsolidated sedimentary deposits above the intact regolith. All variables were standardized by z-scoring their original values. Grid cell i is nested within region (reg = 1, 2, 3, 4). As such, the coefficients  $\beta's$  quantifies the region-specific effect size of the corresponding covariate (explanatory variable) (Fig. 1).

We assigned a hierarchical effect to each of the regolith properties, to estimate region-specific effects ( $\beta$ ) more accurately. The region-specific parameter of a given covariate (denoted by subscript  $\nu$ ;  $\nu=1,2,3,4$ ) is sampled from a common hyperprior distribution, characterized by hyper-parameters  $\mu_{\beta\nu}$  and  $\sigma_{\beta\nu}$  describing the overall effect of that covariate:

$$\beta_{\nu,k} \sim Normal(\mu_{\beta\nu}, \sigma_{\beta\nu})$$
 (6)

where k denotes the region (k=1, 2, 3, 4). The model further includes a random effect term by bedrock lithology  $\varepsilon$  (Eq. 5), indexed by bedrock type (bedrock=1, 2, 3, ..., 15) and region (reg=1, 2, 3, 4), with grid cell i nested within region. This structure of random effect allows us to account for unobservable (or latent) processes associated with different types of bedrock lithology in different regions<sup>35</sup>.

Similar studies of ecosystem sensitivity have standardized ecosystem sensitivity across grids. This is done by standardizing the raw NDVI and raw CWD data in each grid to get a "standardized" slope<sup>87</sup> or by first calculating the raw slope for each grid and then standardizing the raw slopes across grids using grid-specific NDVI distributions and grid-specific CWD distributions<sup>82</sup>. Such standardization was implemented to account for the spatial variation in NDVI (and CWD) magnitude and variance caused by differences in ecosystem types in different grids<sup>82</sup>. With the standardization procedure, ecosystem sensitivity is defined from a relative perspective—focusing on the strength of coupling between CWD variation and NDVI variation. Ecosystem sensitivity in our study is defined from an absolute perspective, capturing the proportional changes in NDVI invoked by one unit change in CWD. To still test whether ecosystem types confound our estimate of the effect of bedrock and its related properties on ecosystem sensitivity, we built a different model, one that also included ecosystem types as an independent predicator:

$$\mu 2_{i} = \beta_{0} + \beta_{1, \text{reg}(i)} Por_{i} + \beta_{2, \text{reg}(i)} Perm_{i} + \beta_{3, \text{reg}(i)} Reg Z_{i} + \beta_{4, \text{reg}(i)} Soil Z_{i} + \varepsilon_{bedrock, \text{reg}(i)} + B_{biom(i)}$$

where B captures the random effect of ecosystem type and biom describes the 14 major terrestrial biomes<sup>42</sup>. Each grid is classified as one of these 14 major biomes. With biomes explicitly included in the model, the multiple regression investigates the relationship between the bedrock-related variables and ecosystem sensitivity, after controlling for ecosystem type. The results of the model with and without ecosystem type controlled for are largely the same (Fig. S8; Supplementary note S1). This suggests that though biome itself might affect ecosystem sensitivity, it does not confound our inference about the relationship between bedrock-related variables and ecosystem sensitivity. Similarly, other climatic variables (e.g., mean annual precipitation, mean annual temperature) might themselves affect ecosystem sensitivity, but they are unlikely to confound our estimate of the effect of bedrock-related variables on ecosystem sensitivity (Table S3).

**Model implementation and fit.** We coded the models in JAGS 4.0.0<sup>88</sup> and implemented them in R<sup>89</sup>, using the RJAGS package. The identifiability problem<sup>90</sup> arising from having an intercept term ( $\beta_0$ ) and the random effect term ( $\epsilon$ ) in Eq. 5 is solved by post-sweeping of random effects<sup>91</sup>. Noninformative priors were used for all the parameters, so the posterior estimates of parameters are informed

principally by the data. For each model, we sampled the posterior parameter space and assessed convergence using 20 parallel Markov chain Monte Carlo (MCMC) chains run for 1000 iterations. We subsequently thinned the chains to produce >3000 approximately independent posterior samples for each parameter of interest. We assessed convergence using the Gelman and Rubin diagnostic<sup>92</sup>. Parameter estimates are reported as the posterior means and 95% credible intervals, defined by the 2.5% and 97.5% percentiles. We evaluated model fit by computing the coefficient of determination ( $R^2$ ) from a regression of observed sensitivity on the predicted sensitivity, given the fitted value for  $\mu_2$  and K (Eqs. 3 and 4) (i.e., using replicated data<sup>92</sup>).

Evaluating model sensitivity to data selection. We evaluated sensitivity of model results to the choice of data used to represent ecosystem productivity. In addition to NDVI, we used the dataset of global monthly average gross primary productivity (GPP; g carbon m<sup>-2</sup> day<sup>-1</sup>) between 1982 and 2016 at the 8 km spatial resolution<sup>93</sup>. GPP in this data product is estimated from the Monteith light use efficiency (LUE) equation optimized in space and time using explicit LUE values derived from selected FLUXNET tower site data<sup>93</sup>. Global gridded GPP was derived using the optimized LUE, Global Inventory Modeling and Mapping Studies (GIMMS3g) canopy fraction of photosynthetically active radiation (FPAR), and Modern-Era Retrospective analysis for Research and Applications (Version 2) (MERRA-2) meteorological information. Annual mean GPP was obtained from the original monthly mean GPP by averaging over 12 months each year. GPP and NDVI show a significantly positive correlation (Fig. S9). Using this independent estimate of GPP, rather than NDVI, to represent ecosystem productivity did not significantly change the major conclusions of this paper, suggesting the observed patterns are robust to data sources (Figs. S3, S4 and S10-12; Supplementary

We also calculated ecosystem sensitivity using growing season NDVI and CWD. We defined growing seasons to be months whose mean monthly temperature is greater than 5 °C94. Annual growing season mean NDVI was calculated by averaging the original monthly mean NDVI over those months. Similarly, we calculated annual growing season CWD, by taking an average of the monthly CWD over the growing season months of a given year between 1982 and 2013. The temperature data used to define growing season were obtained from "Terrestrial Air Temperature and Precipitation: 1900–2014 Gridded Monthly Time Series" provided by the NOAA (PSL, Boulder, Colorado, USA; https://psl.noaa.gov). We then used the same method described above to calculate ecosystem sensitivity, but using growing season NDVI and growing season CWD (Eqs. 1 and 2 above). Using growing season ecosystem sensitivity did not significantly change the major conclusions of this paper, suggesting that the observed patterns are robust to data choices (Figs. S13; Supplementary note S1).

Interpretation of model results. For modeling purposes, the absolute value of sensitivity was log-transformed (Eq. 3). Therefore, positive fitted slopes ( $\beta > 0$ ) imply that the focal variable enhances ecosystem sensitivity, amplifying interannual variability in productivity, while negative slopes suggest that the focal variable reduces ecosystem sensitivity. Interpretations of  $\beta$  vary with region. In regions of negative sensitivity (Region I), broadly characterized as water-limited, we expected that higher water-holding capacity would manifest its strongest effect in dry years (Fig. 1). Thus, in regions of negative sensitivity,  $\beta > 0$  means that as the value of the focal variable increases, productivity will have a larger drop in periods of high CWD. In contrast, in regions of positive sensitivity,  $\beta > 0$  means that as the value of the focal variable increases, productivity will experience greater increases in periods of high CWD. Specifically, in energy-limited regions of positive sensitivity (Region II), water limitation becomes most evident during warming as plant water requirements increase<sup>24</sup>.  $\beta > 0$  means that the focal variable allows a greater increase in productivity with warming (Fig. 1). Likewise, in hyper-arid regions of positive sensitivity (Region IV), water holding capacity likely manifests its strongest effects in dry years (Fig. 1).  $\beta > 0$  means that the focal variable creates conditions that allow a greater increase in productivity with elevated CWD. In contrast, in humid tropical regions of positive sensitivity (those where ecosystem productivity is negatively affected by precipitation<sup>59</sup>; Region III), water-holding capacity likely manifests stronger effects in wetter years (Fig. 1).  $\beta > 0$  means that the focal variable creates conditions that allow stronger productivity increases in drying.

The slopes in the model ( $\beta$ 's) also describe the effect size of corresponding variables. To interpret  $\beta$ 's, we first set all variables at their region-specific mean level, which allows us to estimate a region-specific mean sensitivity; that is,  $|\alpha|=10^{\overline{\mu}2}$  (Eq. 5). When we increase the value of the focal variable by one standard deviation (SD) from its region-specific mean, the sensitivity becomes  $|\alpha|=10^{\overline{\mu}2+\beta_{1,2}\times 1}$  (using Por in Region II as an example). In this case, the effect size of Por (porosity), i.e., the estimated  $\beta_{1,2}$ , can be interpreted as the departure of one SD in the regolith porosity from its mean level results in a change in ecosystem sensitivity in Region II by an amount of  $(10^{\overline{\mu}2+\beta_{1,2}}-10^{\overline{\mu}2})$  or a percent change of  $(10^{\overline{\mu}2+\beta_{1,2}}-10^{\overline{\mu}2})\times 100\%$  relative to its regional mean sensitivity level.

**Model fit.** To evaluate the model fit, we quantified the ability of our model to replicate the 'observed' ecosystem sensitivity (estimated  $\alpha$  in Eq. 2). Model

predicted values fall on the 1:1 line (Fig. S14). Regression of predicted vs observed sensitivity yielded a coefficient of determination  $R^2 = 0.29$ .

## **Data availability**

All the data used in this study are already publicly available with detailed information on their sources provided in the main text. Regardless, a complete set of data has been uploaded to Figshare at: https://doi.org/10.6084/m9.figshare.21078307

## **Code availability**

The R codes to implement statistical models in this study are available from GitHub, https://github.com/xdong05/lithology.

Received: 15 September 2022; Accepted: 24 March 2023; Published online: 12 April 2023

#### References

- Garcia, R. A., Cabeza, M., Rahbek, C. & Araújo, M. B. Multiple dimensions of climate change and their implications for biodiversity. *Science* 344, 1247579 (2014)
- Thomas, C. et al. Extinction risk from climate change. Nature 427, 145–148 (2004).
- Kharin, V. V., Zwiers, F. W., Zhang, X. & Hegerl, G. C. Changes in temperature and precipitation extremes in the IPCC ensemble of global coupled model simulations. *J. Clim* 20, 1419–1444 (2007).
- Seddon, A. W. R., Macias-Fauria, M., Long, P. R., Benz, D. & Willis, K. J. Sensitivity of global terrestrial ecosystems to climate variability. *Nature* 531, 229–232 (2016).
- Scheffer, M. et al. Early-warning signals for critical transitions. Nature 461, 53–59 (2009).
- Abatzoglou, J. T., Dobrowski, S. Z., Parks, S. A. & Hegewisch, K. C. TerraClimate, a high-resolution global dataset of monthly climate and climatic water balance from 1958–2015. Sci. Data 5, 1–12 (2018).
- Hahm, W. J. et al. Bedrock vadose zone storage dynamics under extreme drought: consequences for plant water availability, recharge, and runoff. Water Resour. Res. 58, 1–23 (2022).
- Hahm, W. J., Riebe, C. S., Lukens, C. E. & Araki, S. Bedrock composition regulates mountain ecosystems and landscape evolution. *Proc. Natl. Acad. Sci.* USA 111, 3338–3343 (2014).
- Jiang, Z. et al. Bedrock geochemistry influences vegetation growth by regulating the regolith water holding capacity. Nat. Commun. 11, 1–9 (2020).
- McCormick, E. L. et al. Widespread woody plant use of water stored in bedrock. *Nature* 597, 225–229 (2021).
- Rempe, D. M. & Dietrich, W. E. Direct observations of rock moisture, a hidden component of the hydrologic cycle. *Proc. Natl. Acad. Sci. USA* 115, 2664–2669 (2018).
- Schmidt, L. & Rempe, D. Quantifying dynamic water storage in unsaturated bedrock with borehole nuclear magnetic resonance. *Geophys. Res. Lett.* 47, 1–11 (2020).
- Zhao, J. Rock mass hydraulic conductivity of the Bukit Timah granite, Singapore. Eng. Geol. 50, 211–216 (1998).
- Schild, M., Siegesmund, S., Vollbrecht, A. & Mazurek, M. Characterization of granite matrix porosity and pore-space geometry by in situ and laboratory methods. *Geophys. J. Int.* 146, 111–125 (2001).
- Bazilevskaya, E. et al. Where fast weathering creates thin regolith and slow weathering creates thick regolith. Earth Surf. Process. Landforms 38, 847–858 (2013).
- Graham, R. C., Rossi, A. M. & Hubbert, K. R. Rock to regolith conversion: producing hospitable substrates for terrestrial ecosystems. GSA Today 20, 4–9 (2010).
- Auler, A. S. & Smart, P. L. The influence of bedrock-derived acidity in the development of surface and underground karst: Evidence from the Precambrian carbonates of semi-arid northeastern Brazil. Earth Surf. Process. Landforms 28, 157–168 (2003).
- Holbrook, W. S. et al. Geophysical constraints on deep weathering and water storage potential in the Southern Sierra critical zone observatory. *Earth Surf. Process. Landforms* 39, 366–380 (2014).
- Arkley, R. J. Soil moisture use by mixed conifer forest in a summer-dry climate. Soil Sci. Soc. Am. J. 45, 423–427 (1981).
- Witty, J. H., Graham, R. C., Hubbert, K. R., Doolittle, J. A. & Wald, J. A. Contributions of water supply from the weathered bedrock zone to forest soil quality. *Geoderma* 114, 389–400 (2003).

- Jones, D. P. & Graham, R. C. Water-holding characteristics of weathered granitic rock in chaparral and forest ecosystems. Soil Sci. Soc. Am. J. 57, 256–261 (1993).
- Amundson, R., Heimsath, A., Owen, J., Yoo, K. & Dietrich, W. E. Hillslope soils and vegetation. Geomorphology 234, 122–132 (2015).
- Schwinning, S. The ecohydrology of roots in rocks. Ecohydrology 3, 238–245 (2010).
- Dolezal, J., Kurnotova, M., Stastna, P. & Klimesova, J. Alpine plant growth and reproduction dynamics in a warmer world. New Phytol. 228, 1295–1305 (2020).
- Zhang, K. et al. Satellite-based model detection of recent climate-driven changes in northern high-latitude vegetation productivity. J. Geophys. Res. Biogeosci. 113, G3 (2008).
- Intergovernmental Panel on Climate Change (IPCC). Climate Change 2007: The Scientific Basis. Contribution of Working Group I to the Fourth Assessment Report of the Intergovernmental Panel on Climate Change. Cambridge University Press. (2007). https://doi.org/10.1029/2007GL030749.
- Porder, S., Hilley, G. E. & Chadwick, O. A. Chemical weathering, mass loss, and dust inputs across a climate by time matrix in the Hawaiian Islands. *Earth Planet. Sci. Lett.* 258, 414–427 (2007).
- Castle, S. C. & Neff, J. C. Plant response to nutrient availability across variable bedrock geologies. *Ecosystems* 12, 101–113 (2009).
- Gerdol, R., Marchesini, R. & Iacumin, P. Bedrock geology interacts with altitude in affecting leaf growth and foliar nutrient status of mountain vascular plants. J. Plant Ecol. 10, 839–850 (2017).
- Brady, K. U., Kruckeberg, A. R. & Bradshaw, H. D. Evolutionary ecology of plant adaptation to serpentine soils. *Annu. Rev. Ecol. Evol. Syst.* 36, 243–266 (2005).
- 31. von Liebig, J. Die grundsätze der agricultur-chemie mit rücksicht auf die in england angestellten untersuchungen. Vieweg, Braunschweig (1855).
- Hahm, W. J. et al. Lithologically controlled subsurface critical zone thickness and water storage capacity determine regional plant community composition. Water Resour. Res. 55, 3028–3055 (2019).
- Hartmann, J. & Moosdorf, N. The new global lithological map database GLiM: a representation of rock properties at the Earth surface. *Geochem. Geophys. Geosyst.* 13, 1–37 (2012).
- Gleeson, T., Moosdorf, N., Hartmann, J. & Van Beek, L. P. H. A glimpse beneath earth's surface: GLobal HYdrogeology MaPS (GLHYMPS) of permeability and porosity. *Geophys. Res. Lett.* 41, 6298–6305 (2014).
- Pelletier, J. D. et al. A grided global data set of soil, intact regolith, and sedimentary deposit thickness for regional and global land surface modeling. J. Adv. Model. Earth Syst. 6, 1339–1350 (2015).
- Pinzon, J. E. & Tucker, C. J. A non-stationary 1981–2012 AVHRR NDVI3g time series. *Remote Sens.* 6, 6929–6960 (2014).
- 37. Park, H. et al. Nonlinear response of vegetation green-up to local temperature variations in temperate and boreal forests in the Northern Hemisphere. *Remote Sens. Environ.* **165**, 100–108 (2015).
- Harvey, J. E. et al. Tree growth influenced by warming winter climate and summer moisture availability in northern temperate forests. *Glob. Chang. Biol.* 26, 2505–2518 (2020).
- Lindroth, A., Grelle, A. & Morén, A. S. Long-term measurements of boreal forest carbon balance reveal large temperature sensitivity. Glob. Chang. Biol. 4, 443–450 (1998).
- Díaz, S., Cabido, M., Zak, M., Martínez Carretero, E. & Araníbar, J. Plant functional traits, ecosystem structure and land-use history along a climatic gradient in central-western Argentina. J. Veg. Sci. 10, 651–660 (1999).
- Schuchardt, M. A., Berauer, B. J., von Heßberg, A., Wilfahrt, P. & Jentsch, A. Drought effects on montane grasslands nullify benefits of advanced flowering phenology due to warming. *Ecosphere* 12, e03661 (2021).
- 42. Dinerstein, E. et al. An ecoregion-based approach to protecting half the terrestrial realm. *Bioscience* **67**, 534–545 (2017).
- Martin-Benito, D. & Pederson, N. Convergence in drought stress, but a divergence of climatic drivers across a latitudinal gradient in a temperate broadleaf forest. J. Biogeogr. 42, 925–937 (2015).
- Quetin, G. R. & Swann, A. L. S. Empirically derived sensitivity of vegetation to climate across global gradients of temperature and precipitation. J. Clim. 30, 5835–5849 (2017).
- Huxman, T. E. et al. Convergence across biomes to a common rain-use efficiency. Nature 429, 651–654 (2004).
- Fensholt, R. et al. Greenness in semi-arid areas across the globe 1981–2007 an Earth observing satellite based analysis of trends and drivers. *Remote Sens. Environ.* 121, 144–158 (2012).
- 47. Andela, N., Liu, Y. Y., Van Dijk, A. I. J. M., De Jeu, R. A. M. & McVicar, T. R. Global changes in dryland vegetation dynamics (1988–2008) assessed by satellite remote sensing: Comparing a new passive microwave vegetation density record with reflective greenness data. *Biogeosciences* 10, 6657–6676 (2013).

- Donohue, R. J., Roderick, M. L., McVicar, T. R. & Farquhar, G. D. Impact of CO2 fertilization on maximum foliage cover across the globe's warm, arid environments. *Geophys. Res. Lett.* 40, 3031–3035 (2013).
- Dürr, H. H., Meybeck, M. & Dürr, S. H. Lithologic composition of the Earth's continental surfaces derived from a new digital map emphasizing riverine material transfer. Glob. Biogeochem. Cycles 19, 1–23 (2005).
- Thuiller, W., Lavorel, S. & Araújo, M. B. Niche properties and geographical extent as predictors of species sensitivity to climate change. *Glob. Ecol. Biogeogr.* 14, 347–357 (2005).
- Isbell, F. et al. Biodiversity increases the resistance of ecosystem productivity to climate extremes. Nature 526, 574–577 (2015).
- 52. Oliveira, B. F., Moore, F. C. & Dong, X. Biodiversity mediates ecosystem sensitivity to climate variability. *Commun. Biol.* 5, 103–116 (2022).
- Kroël-Dulay, G. et al. Increased sensitivity to climate change in disturbed ecosystems. Nat. Commun. 6, 1–7 (2015).
- Hoylman, Z. H. et al. Hillslope topography mediates spatial patterns of ecosystem sensitivity to climate. *J. Geophys. Res. Biogeosciences* 123, 353–371 (2018).
- Smith, T. J. et al. Small soil storage capacity limits benefit of winter snowpack to upland vegetation. Hydrol. Process. 25, 3858–3865 (2011).
- Heilman, J. L. et al. Water-storage capacity controls energy partitioning and water use in karst ecosystems on the Edwards Plateau. *Texas. Ecohydrology* 7, 127–138 (2014).
- Fu, R. Global warming-accelerated drying in the tropics. Proc. Natl. Acad. Sci. USA 112, 3593–3594 (2015).
- Neelin, J. D., Münnich, M., Su, H., Meyerson, J. E. & Holloway, C. E. Tropical drying trends in global warming models and observations. *Proc. Natl. Acad.* Sci. USA 103, 6110–6115 (2006).
- Schuur, E. A. G. Productivity and global climate revisited: The sensitivity of tropical forest growth to precipitation. *Ecology* 84, 1165–1170 (2003).
- Schuur, E. A. G. The effect of water on decomposition dynamics in mesic to wet Hawaiian montane forests. *Ecosystems* 4, 259–273 (2001).
- Schuur, E. A. & Matson, P. A. Net primary productivity and nutrient cycling across a mesic to wet precipitation gradient in Hawaiian montane forest. *Oecologia* 128, 431–442 (2001).
- Davidson, E. A., Nepstad, D. C., Ishida, F. Y. & Brando, P. M. Effects of an experimental drought and recovery on soil emissions of carbon dioxide, methane, nitrous oxide, and nitric oxide in a moist tropical forest. *Glob. Chang. Biol.* 14, 2582–2590 (2008).
- Black, T. A. et al. Increased carbon sequestration by a Boreal deciduous forest in years with a warm spring. *Geophys. Res. Lett.* 27, 1271–1274 (2000).
- Allison, S. D. & Treseder, K. K. Warming and drying suppress microbial activity and carbon cycling in boreal forest soils. *Glob. Chang. Biol.* 14, 2898–2909 (2008).
- Lian, X. et al. Multifaceted characteristics of dryland aridity changes in a warming world. Nat. Rev. Earth Environ. 2, 232–250 (2021).
- Hickler, T. et al. Precipitation controls Sahel greening trend. Geophys. Res. Lett. 32, 1–4 (2005).
- Huber, S., Fensholt, R. & Rasmussen, K. Water availability as the driver of vegetation dynamics in the African Sahel from 1982 to 2007. *Glob. Planet. Change* 76, 186–195 (2011).
- Wei, F. et al. African dryland ecosystem changes controlled by soil water. L. Degrad. Dev. 30, 1564–1573 (2019).
- Porder, S. & Ramachandran, S. The phosphorus concentration of common rocks-a potential driver of ecosystem P status. Plant Soil 367, 41–55 (2013).
- Morford, S. L., Houlton, B. Z. & Dahlgren, R. A. Geochemical and tectonic uplift controls on rock nitrogen inputs across terrestrial ecosystems. *Global Biogeochem. Cycles* 30, 333–349 (2016).
- Porder, S. How Plants enhance weathering and how weathering is important to plants. *Elements* 15, 241–246 (2019).
- Turner, B. L., Brenes-Arguedas, T. & Condit, R. Pervasive phosphorus limitation of tree species but not communities in tropical forests. *Nature* 555, 367–370 (2018).
- Rahbek, C. et al. Building mountain biodiversity: geological and evolutionary processes. Science 365, 1114–1119 (2019).
- Myneni, R. B. et al. Global products of vegetation leaf area and fraction absorbed PAR from year one of MODIS data. *Remote Sens. Environ.* 83, 214–231 (2002).
- Huete, A. et al. Overview of the radiometric and biophysical performance of the MODIS vegetation indices. Remote Sens. Environ. 83, 195–213 (2002).
- Glenn, E. P., Huete, A. R., Nagler, P. L. & Nelson, S. G. Relationship between remotely-sensed vegetation indices, canopy attributes and plant physiological processes: What vegetation indices can and cannot tell us about the landscape. Sensors 8, 2136–2160 (2008).
- Guanter, L. et al. Retrieval and global assessment of terrestrial chlorophyll fluorescence from GOSAT space measurements. *Remote Sens. Environ.* 121, 236–251 (2012).

- Tucker, C. J. et al. An extended AVHRR 8-km NDVI dataset compatible with MODIS and SPOT vegetation NDVI data. *Int. J. Remote Sens.* 26, 4485–4498 (2005).
- 79. Willmott, C. J., Rowe, C. M. & Mintz, Y. Climatology of the terrestrial seasonal water cycle. *J. Climatol.* 5, 589–606 (1985).
- 80. Dobrowski, S. Z. et al. The climate velocity of the contiguous United States during the 20th century. *Glob. Chang. Biol.* **19**, 241–251 (2013).
- Mitchell, P. J. et al. An ecoclimatic framework for evaluating the resilience of vegetation to water deficit. Glob. Chang. Biol. 22, 1677–1689 (2016).
- 82. Hoylman, Z. H. et al. The topographic signature of ecosystem climate sensitivity in the Western United States. *Geophys. Res. Lett.* **46**, 14508–14520 (2010)
- Samuels-Crow, K. E., Ogle, K. & Litvak, M. E. Atmosphere-soil interactions govern ecosystem flux sensitivity to environmental conditions in semiarid woody ecosystems over varying timescales. *J. Geophys. Res. Biogeosci.* 125, 1–16 (2020).
- Gleeson, T. et al. Mapping permeability over the surface of the Earth. Geophys. Res. Lett. 38, 1–6 (2011).
- Bernabé, Y., Mok, U. & Evans, B. Permeability-porosity relationships in rocks subjected to various evolution processes. *Pure Appl. Geophys.* 160, 937–960 (2003).
- Ogle, K., Liu, Y., Vicca, S. & Bahn, M. A hierarchical, multivariate metaanalysis approach to synthesising global change experiments. *New Phytol.* 231, 2382–2394 (2021).
- Tai, X. et al. Hillslope hydrology influences the spatial and temporal patterns of remotely sensed ecosystem productivity. Water Resour. Res. 56, 1–13 (2020).
- 88. Plummer, M. JAGS: a program for analysis of bayesian graphical models using gibbs sampling. *Proceedings of the 3rd International Workshop on Distributed Statistical Computing (DSC 2003)* **124**, 1–10 (2003).
- R Core Team. R: A language and environment for statistical computing. R Foundation for Statistical Computing (2021). https://doi.org/10.1002/jpln. 19801430513.
- Raue, A., Kreutz, C., Theis, F. J. & Timmer, J. Joining forces of Bayesian and frequentist methodology: a study for inference in the presence of nonidentifiability. *Philos. Trans. R. Soc. A Math. Phys. Eng. Sci.* 371, 20110544 (2013).
- Ogle, K. & Barber, J. J. Ensuring identifiability in hierarchical mixed effects Bayesian models. Ecol. Appl. 30, 1–19 (2020).
- Gelman, A. & Rubin, D. B. Inference from iterative simulation using multiple sequences. Stat. Sci. 7, 457–511 (1992).
- Madani, N. & Parazoo, N. C. Global Monthly GPP from an Improved Light Use Efficiency Model, 1982–2016. (ORNL DAAC, 2020).
- Menzel, A., Jakobi, G., Ahas, R., Scheifinger, H. & Estrella, N. Variations of the climatological growing season (1951–2000) in Germany compared with other countries. *Int. J. Climatol.* 23, 793–812 (2003).

## **Acknowledgements**

This work is supported by the National Science Foundation (EAR-1905259 'CZ-RCN: Research Coordination in Carbonate Critical Zones') awarded to JBM, and by the National Science Foundation (DEB-1924378: 'CNH2-S: Understanding the Coupling Between Climate Policy and Ecosystem Change') awarded to X.D. This work is also supported by the National Natural Science Foundation of China (52109046) to T.T.

## **Author contributions**

X.D., J.M., M.C., and T.T. conceived the research idea, and X.D. developed the statistical models. T.T. collected and compiled datasets. All authors discussed the results and contributed to the preparation of the manuscript.

## **Competing interests**

The authors declare no competing interests.

## **Additional information**

**Supplementary information** The online version contains supplementary material available at https://doi.org/10.1038/s43247-023-00773-x.

Correspondence and requests for materials should be addressed to Tongbi Tu.

Peer review information Communications Earth & Environment thanks the anonymous reviewers for their contribution to the peer review of this work. Primary Handling Editor: Ioe Aslin.

Reprints and permission information is available at http://www.nature.com/reprints

**Publisher's note** Springer Nature remains neutral with regard to jurisdictional claims in published maps and institutional affiliations.

Open Access This article is licensed under a Creative Commons Attribution 4.0 International License, which permits use, sharing, adaptation, distribution and reproduction in any medium or format, as long as you give appropriate credit to the original author(s) and the source, provide a link to the Creative Commons license, and indicate if changes were made. The images or other third party material in this article are included in the article's Creative Commons license, unless indicated otherwise in a credit line to the material. If material is not included in the article's Creative Commons license and your intended use is not permitted by statutory regulation or exceeds the permitted use, you will need to obtain permission directly from the copyright holder. To view a copy of this license, visit <a href="https://creativecommons.org/licenses/by/4.0/">https://creativecommons.org/licenses/by/4.0/</a>.

© The Author(s) 2023